JNEST EISSN: 2961-8738 ● PISSN: 2961-8916 ● DOI: 10.56741/jnest.v3i03.569
Article Received 16 April 2024. Revised 7 June 2024.

Transparent Film Profiling and Analysis by White Light Scanning Interferometry

Nway Nway Hlaing, Lei Lei Yin Win, Hla Myo Tun*, Devasis Pradhan

***Abstract*—This paper describes the use of white light scanning interferometry with a Super luminescent diode (SLD) for thin film surface measurement. The technique provides 3D top surface and thickness profiles of transparent films, as well as detailed properties of multilayer film stacks, including material optical properties. The setup involves splitting a laser beam with a beam splitter, generating interference signals detected by a photodetector, and then converting analog signals to digital using an A/D converter for further analysis with LabView and MATLAB software. In this paper, the theoretical analysis and simulation study of white light scanning interferometry for transparent film measurement is discussed. This approach offers a flexible tool for both engineering and structured surface measurements.**

***Index Terms*— Interferometry, Semiconductor Structure, Surface Profile, Thin Film Measurement, WLSI.**

I. Introduction

EFFECTIVE measurements of film thickness and refractive index of the films are important factors that determine the function and performance of a coated device. Conventionally the film thickness and refractive index are measured by spectral photometry or ellipsometry methods [1, 2]. Both methods can only measure film thickness at the sampling points. Recently, scanning white light interferometry has been extended in its application from surface measurement to film thickness measurement. It can measure the surface finishes of a film as well as film thickness over the whole measurement field [3-5]. To perform the measurements quickly and efficiently is one of the key issues for realizing a sustained, controlled fusion reaction. In most cases, thin film measurement methods using optical interferometry are only interested in film thickness measurement [6].

The interference signals are created by the two interfaces of the film. It cannot satisfy the above demands. White light scanning interferometry (WSI) is an effective method for surface measurement of engineering surfaces and structured surfaces [7]. The paper highlights that in current surface metrology applications, white light scanning interferometry primarily deals with surfaces reflecting only from the uppermost layer. However, when measuring transparent thin films, interference from both the top and bottom surfaces, as well as between the two surfaces, complicates measurements. Effective separation of these interference signals is crucial for successful measurement. Through extensive frequency-domain analysis, the paper proposes a method to separate and reconstruct these signals, enabling the measurement of both top and bottom surface finishes, along with generating a precise film thickness map [8].

In this paper, a method to measure the thickness of thin film using white light scanning interferometry was proposed. To calculate the phase and amplitude error value resulting from optical interference between the top and bottom surfaces of the thin film will determined from white light-scanning interferometry. Recent rapid advances in electronics and computer technology now allow the incorporation of newly developed, sophisticated algorithms in interferometric profilers, with dramatic results. By using the proposed method, it will become possible to measure the thickness of the thin film simultaneously with reducing cost and time.

Nway Nway Hlaing and **Lei Lei Yin Win** are with the Department of Electronic Engineering of Yangon Technological University (YTU), Gyogone, Insein PO, 11011, Yangon, Myanmar. **Prof. Dr. Hla Myo Tun** (Corresponding atuhor) is with the Research Department of Yangon Technological University (YTU), and King Lauk Phya Institute of Technology Myaungmya, Ayeyawaddy Region, Republic of the Union of Myanmar. (Corresponding email: ecdepartment.ytu@gmail.com.). **Prof. Dr. Devasis Pradhan** is with the Acharya Institute of Technology in India.

II. Overall System Description

Figure 1 depicts the block diagram of the sinusoidal phase modulating interferometer. Its main components include a Superluminescent Diode (SLD) with an SLD driver, an acousto-optic tunable filter (AOTF) with an AOTF driver, a beam splitter, a mirror, and a thin film. Initially, the SLD is powered by the SLD driver, which requires three types of DC power supply. The SLD emits white light directed towards the acousto-optic tunable filter (AOTF). The AOTF, controlled by the AOTF driver requiring modulation and frequency from two types of DC power supply, interacts with the light. The system operates on the sinusoidal phase modulating interferometry method and utilizes Wavelength Scanning Interferometry (WSI), a two-dimensional signal processing technique. In this setup, the light source is an SLD, and the interference signal it generates is detected by a charged-coupled device (CCD).

The selected light wavelength is determined by

$$\lambda = \Delta n \alpha \propto \frac{V_a}{f_a} \quad \text{..... (1)}$$

where Δn is the birefringence of the crystal used as the diffraction material, α is a complex parameter dependent on the design of the AOTF. Va and fa are the velocity and frequency of the acoustic wave, respectively. The wavelength of the light that is selected by this diffraction can therefore be varied simply by changing the driving frequency, fa. As a result, different wavelengths of light will pass through the AOTF in sequence so that a series of interferograms of different wavelengths will be detected by the CCD. The absolute optical path difference (OPD) is given by

© 2024 IISTR

$$h(x,y)=\frac{\Delta(x,y,\Delta k)}{(2\pi\Delta k)} \quad \text{..... (2)}$$

where h(x, y) is the OPD on pixel (x, y) , and k is the wave number which is the reciprocal of the wavelength. It can be calculated in real-time by analyzing the interferogram captured by the CCD using FFT analysis or convolution [7-8].

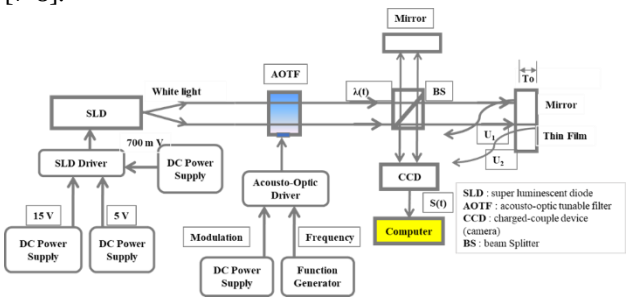


Fig. 1. Schematic Diagram of WLSI System

III. Measurement Principle

A. White light scanning interferometry

The light source mentioned is a Superluminescent Diode (SLD). SLDs are commonly used in Optical Coherence Tomography (OCT) due to their broad bandwidth and coherence properties, allowing for high-resolution imaging. By measuring the interference patterns, OCT can extract information about the optical path length of the light in different regions of the sample. A CCD (Charge-Coupled Device) camera is typically used to capture the interference patterns. The camera detects the intensity of the interfered light, allowing for the creation of high-resolution images [9-11]. The combination of SLD, CCD camera detection, and two-dimensional signal processing contributes to the effectiveness of OCT in capturing detailed structural information from a variety of materials and biological tissues in Fig.2.

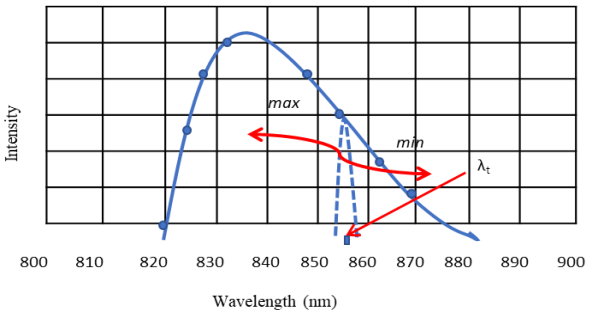


Fig. 2. Optical Oscillation Spectrum of SLD

$$\psi(t)=-2\pi\left(\Delta\lambda t/\lambda_0^2\right)L+\left(2\pi/\lambda_0\right) \quad \text{.....(3)}$$

$$\lambda(t)=\lambda_c+\Delta\lambda(t) \quad \text{.....(4)}$$

The white light scanning method is likely applied in the context of optical interferometry, where interference patterns are sensitive to changes in the film's thickness or refractive index. By isolating the signals associated with different surfaces through Fast Fourier Transform (FFT) analysis and filtering, researchers can extract valuable information about the individual topographies of the film's surfaces. Fig.3 illustrates the analysis method employed for separating the two surfaces of the film and reconstructing their profiles. Initially, Fast Fourier Transform (FFT) analysis identifies the two dominant frequencies present in the captured data. Subsequently, the captured data undergo filtering using two band-pass filters tailored to the FFT analysis results. By applying these filters to the measured signal, interference signals between the reference mirror and both the top and bottom surfaces of the film can be isolated. These separated signals facilitate the reconstruction of surface topographies for both the top and bottom surfaces of the film.

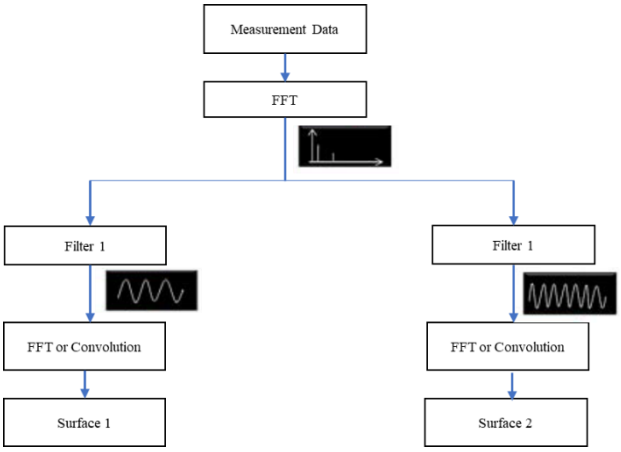


Fig. 3. Data processing chart to separate and reconstruct the two film surfaces.

B. Simulations for Thickness Measurements of thin films

Fig. 4 describes the wide spectrum of the Super luminescent diode (SLD) filtered using an Acousto-Optic Tunable Filter (AOTF). This type of filter uses sound waves (acoustic waves) to diffract and shift the wavelength of light, allowing you to select a specific range of wavelengths. The wide spectrum of the SLD is filtered using an Acousto-Optic Tunable Filter (AOTF). This type of filter uses sound waves (acoustic waves) to diffract and shift the wavelength of light, allowing you to select a specific range of wavelengths. Wavelength parameters are central wavelength (λc): 840nm and wavelength scanning width (2b): 13nm (which implies b=6.5nm).

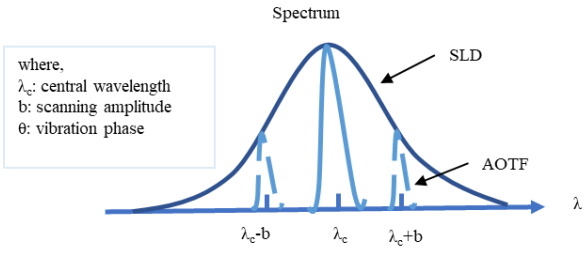


Fig. 4. Wide Spectrum of Super luminescent diode (SLD)

To obtain the amplitude of the modulation Z_b and the phase α from the white light scanning signal

$S(t)= \cos[2\pi(2T/\lambda(t))]$ ..... (5)

$S(t)= \cos[2\pi(2T)/(\lambda_C+\Delta\lambda)]$ ..... (6)

Since $1/(\lambda_C+\Delta\lambda) \cong (1/\lambda_C)(1-\Delta\lambda/\lambda_C)$ $(\Delta\lambda/\lambda_C<<1)$

$= (1/\lambda_C)-(\Delta\lambda/\lambda_C^2)$ ..... (7)

$Z_b = 2\pi(b/\lambda_C^2)(2T)$ ..... (8)

$\alpha = 2\pi(2T/\lambda_C)$ ..... (9)

From these values, the optical path difference (OPD) L. But the measured phase αm is wrapped within –π and π at optical thickness T=nT$_0$ where n is the refractive index.

IV. Measurement Results

It seems like a study or experiment involving the measurement and analysis of a thin film coated onto a glass substrate has been described. The experiment involves measuring interferograms on different points of the film surface and the glass substrate and then analyzing these signals to reconstruct the surfaces of the film.

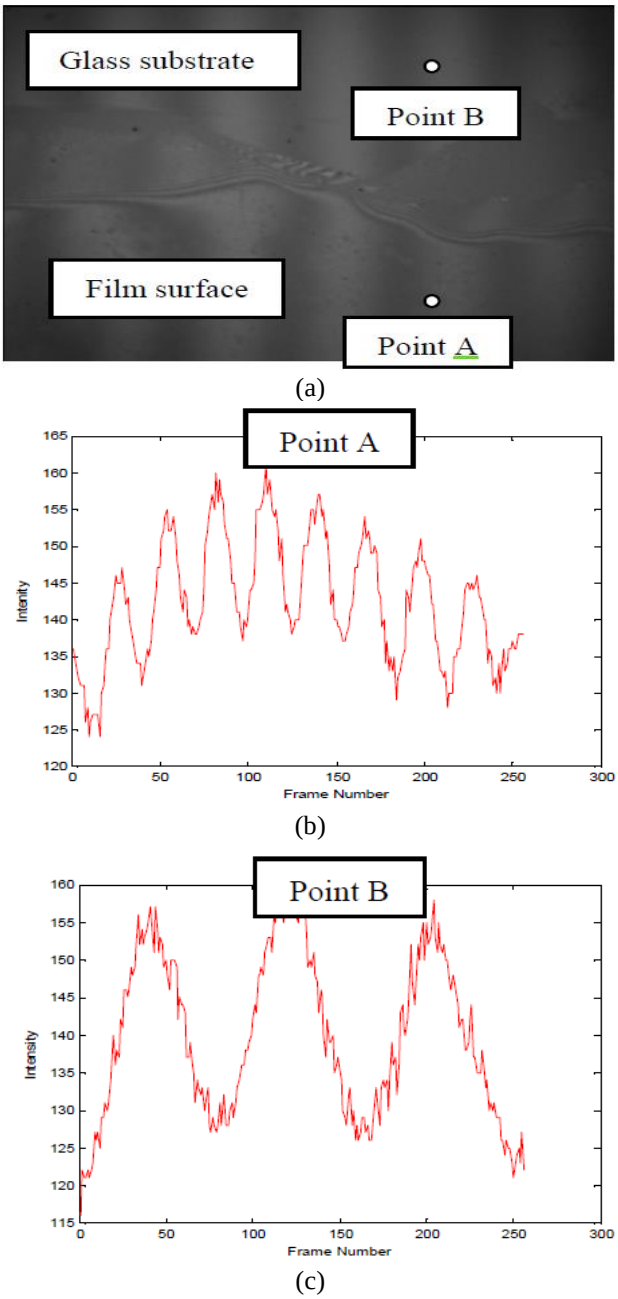


Fig.5. (a) measured image of the sample surface; (b) interferogram on the film surface; (c) interferogram on a glass substrate.

Fig. 5(a) likely shows the measured image of the edge of the step of the coating film on the glass substrate. Fig. 5(b) displays the interferogram on point A of the thin film surface, containing interference information between the reference mirror and the two film surfaces. Finally, Fig. 5(c) depicts the interferogram on point B of the glass substrate. It appears that the experiment aims to characterize the topography or thickness profile of the thin film on the glass substrate using interferometric techniques. This information could be valuable for various applications, such as quality control in thin film fabrication processes or understanding the behavior of dielectric materials in optical systems.

V. Experimental Measurement Result Of Amplitude, Phase And Θ

Table 1 shows the interference signal is described by the equation S(t) is A+Bcos [Zcos($2\pi f_c t+\theta$) +α], the sinusoidal waveform acos ($2\pi f_c t$) is applied to the PZT with carrier frequency 580 Hz and PZT is adjusted by applying a DC offset voltage and amplitude by the function generator. Also, the different values of the amplitude of the phase modulation Z_b, the phase α, and θ are obtained by changing the received analog signal into a digital signal with an A/D converter, capturing the digital signal with LabView software, and simulating with MATLAB software. With the wavelength λ=840nm, the optical path difference L= 60μm, the phase α=(2π/λ) L and the amplitude Z= (4π/ λ).

TABLE I
EXPERIMENTAL MEASUREMENT RESULT OF AMPLITUDE Z, PHASE A, AND Θ

Amplitude	DC offset	Z	α	θ
4V	2V	2.24	-1.6	-0.23
4V	2V	2.37	1.75	2.87
5V	2V	2.80	1.41	-2.09

According to the theoretical value, try to get a similar result with the set-up measurement by controlling the amplitude voltage and DC offset voltage in the oscilloscope as shown in Table 2.

TABLE II
EXPERIMENTAL RESULT OF Z1, Z2 AND ALPHA= 0

Amplitude 4.29V, DC offset 1V, Alpha = 0 rad		
Alpha	Z_1	Z_2
-3.05931	3.291	3.2787
3.07196	3.499	3.2378
-3.00309	3.336	3.2997
-2.81948	3.346	3.2737
2.904607	3.337	3.2932

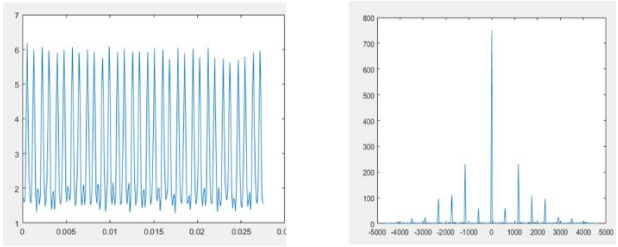


Fig. 6. (a) Interference signal, (b) Fast Fourier Transform of interference signal

TABLE III
EXPERIMENTAL RESULT OF Z1, Z2, AND ALPHA=.4

Amplitude 4.29V, DC offset 1.7V, Alpha = 0.4 rad		
Alpha	Z_1	Z_2
0.5759	3.3120	3.2635
0.3787	3.4700	3.3009
0.4832	3.3250	3.3927
0.3760	3.3440	3.3196
0.3190	3.4390	3.2308

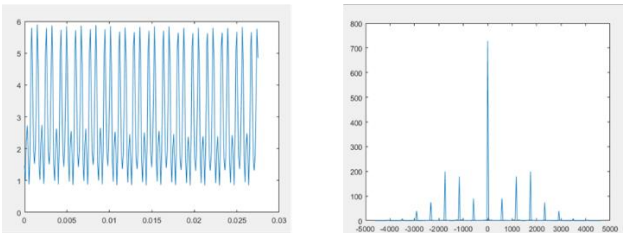


Fig. 7. (a) Interference signal, (b) Fast Fourier Transform of interference signal

TABLE III
EXPERIMENTAL RESULT OF Z1, Z2, AND ALPHA=.8

Amplitude 4.29V, DC offset 1.6V, Alpha = 0.8 rad		
Alpha	Z_1	Z_2
0.7865	3.3870	3.3719
0.7750	3.3190	3.3364
0.7926	3.4170	3.3269
0.7758	3.3620	3.2988
0.8671	3.3610	3.3803

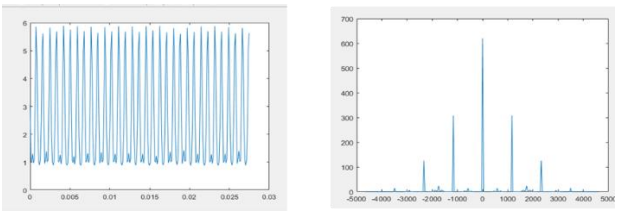


Fig. 8. (a) Interference signal, (b) Fast Fourier Transform of interference signal

TABLE III
EXPERIMENTAL RESULT OF Z1, Z2, AND ALPHA=1.2

Amplitude 4.29V, DC offset 1.2V, Alpha = 1.2 rad		
Alpha	Z_1	Z_2
1.0847	3.3980	3.2375
1.1546	3.3490	3.3459
1.1334	3.3400	3.3919
1.1462	3.3700	3.4520
1.0168	3.3300	3.2003

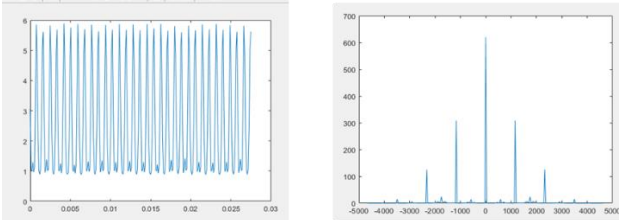


Fig. 9. (a) Interference signal, (b) Fast Fourier Transform of interference signal

TABLE IV
EXPERIMENTAL RESULT OF Z1, Z2, AND ALPHA=1.5

Amplitude 4.29V, DC offset 1.8V, Alpha = 1.5 rad		
Alpha	Z_1	Z_2
1.6922	3.3510	3.5845
1.5212	3.3730	4.2546
1.7191	3.3220	3.8355
1.5339	3.3480	1.9658
1.5252	3.3770	4.4100

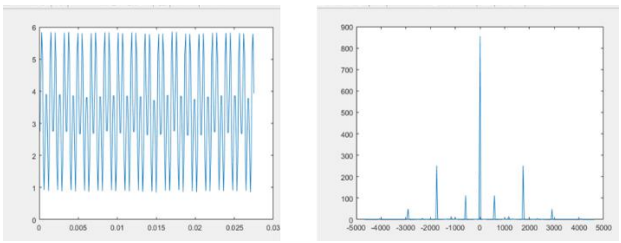


Fig. 10. (a) Interference signal, (b) Fast Fourier Transform of interference signal

At a specific radial position (z=3.4 rad), the parameter alpha is varied from 0 to π/2 radians. The intervals between each change in alpha are specified to be 0.4 radians. There is a change in amplitude bias associated with changes in the radial position (z). The specific relationship between amplitude bias and z is not detailed. The DC offset bias changes as alpha varies. Again, the specific relationship between DC offset bias and alpha is not provided. The changes in amplitude bias with radial position (z) and DC offset bias with alpha variations suggest a systematic exploration of the system's behavior under different conditions in Fig. 6. to Fig. 10.

TABLE V
RESULTS OF THE THICKNESS OF THE THIN FILM OF THE Z1, Z2, AND THE ERRORS WITHOUT NOISE

α	α_result	Z_1-result	Z_2-result	Z_1error	Z_2error
$2\pi(2T/\lambda_c)$	2.6928	3.4700	3.4700	0.0028	0.0028
0	6.2361×10^{-16}	2.9300	3.4700	0.5428	0.0028
π/2	1.5708(π/2)	3.4700	3.5000	0.0028	0.0272
π/4	0.7853(π/4)	3.4700	3.4700	0.0028	0.0028
3π/2	-1.5707(-π/2)	3.4700	3.5000	0.0028	0.0272

Tables VI and VII show the calculation of the thickness of the thin film by using theoretical values. To calculate the thickness of the thin film, the signal components Z and α are very important. It seems like provided a detailed explanation of the calculation process for determining the thickness of a thin film using theoretical values. The steps involve examining signal components Z and α and then calculating the minimum error values of Z1 and Z2 at various values of α. After determining the optimal values for Z1 and Z2, the optical path difference L and error value are calculated, leading to the final thickness estimation of the thin film.

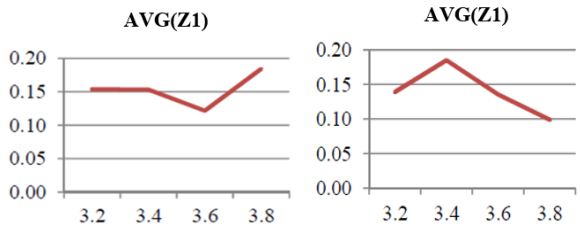
Table V shows values likely represent the overall error associated with signal components Z1 and Z2 for different Z values. The total average error could be a measure of how well the theoretical or experimental values of Z1 and Z2 match the expected or desired values.

TABLE VI
CALCULATION OF THE OPTICAL PATH DIFFERENCE (L), THICKNESS (TO), AND TO ERRORS WITHOUT NOISE

α	α_result	L_result µm	L_error µm	T_o_result µm	T_o error µm
$2\pi(2T/\lambda_c)$	2.6928	60	0.10611	20	1.0889×10^{-15}
0	6.2361×10^{-16}	50.400	9.5999	16.800	3.2000
$\pi/2$	$1.5708(\pi/2)$	59.850	0.14989	19.950	0.0500
$\pi/4$	$0.7853(\pi/4)$	59.744	0.2548	19.9149	0.085
$3\pi/2$	-1.5707 $(-\pi/2)$	60.270	0.27011	20.09	0.0900

TABLE VII
EXPERIMENTAL RESULT OF Z1, Z2, AND ALPHA=.4
TOTAL AVERAGE ERROR VALUE OF Z1, Z2 FOR Z=3.2, Z=3.4, Z=3.6 AND Z=3.8

Z	AVERAGE (EZ_1)	AVERAGE (EZ_2)
3.2	0.15	0.14
3.4	0.15	0.18
3.6	0.12	0.14
3.8	0.18	0.10



(a) (b)

Fig. 11. Average error of Z1 and Z2 values and alpha curves

Fig. 11(a) shows the average error of Z1 value and alpha curve. Here, the graph shows how the average error (EZ1) changes with different alpha values (3.2 to 3.8). The x-axis represents different values of alpha, ranging from 3.2 to 3.8. The y-axis represents the average error, ranging from 0.00 to 0.20. At alpha = 3.2, the average error is approximately 0.15. The average error remains roughly constant from alpha = 3.2 to alpha = 3.4. From alpha = 3.4 to alpha = 3.6, there is a slight decrease in the average error, dropping below 0.15. After alpha = 3.6, the average error increases again, reaching around 0.17 at alpha = 3.8. There is a slight dip in the average error around alpha = 3.6, indicating that this might be a more optimal value for minimizing the error compared to the other alpha values in the range shown. The average error does not change drastically over the range of alpha values, suggesting some level of stability in the system being analyzed.

The graph in Figure 11(b) shows how the average error (EZ2) changes with different alpha values (3.2 to 3.8). The x-axis represents different values of alpha, ranging from 3.2 to 3.8. The y-axis represents the average error, ranging from 0.00 to 0.20. At alpha = 3.2, the average error is approximately around 0.15. The error peaks around 0.18 at alpha = 3.4, indicating this is the least optimal point in the given range. After alpha = 3.6, the error drops to around 0.12. The error continues to drop, falling just below 0.10, suggesting this is the most optimal point for minimizing error within the range. This indicates a non-linear relationship between alpha and the average error of Z1 suggesting that there is an optimal range for alpha where the error is minimized. The graph helps in identifying the point where the error is at its highest and can be used to avoid such values of alpha in practical applications to maintain lower error rates.

V. DISCUSSIONS

The findings presented in this study have substantial implications for the advancement of measurement techniques in the field of thin film characterization. By leveraging white light scanning interferometry, the proposed method successfully achieves precise measurements of thin film thickness, addressing a critical need in various scientific and industrial applications. Moreover, the study's examination of amplitude error values in the presence of random noise reveals that the introduced errors were random, suggesting that improvements in environmental control could further enhance measurement accuracy. Despite these challenges, the method demonstrated robust performance, effectively measuring the thickness of a transparent plate with a thin film on its surface.

The ability to simultaneously measure the surface shape and thickness of thin films is a notable breakthrough, offering significant practical benefits. This dual measurement capability can lead to reduced costs and time in the characterization process, making the method highly advantageous for industries where time-efficient and cost-effective measurements are crucial. Overall, these findings advance the field by providing a validated, efficient, and accurate technique for thin film measurement, potentially setting a new standard for future research and applications in material science and related disciplines.

VI. CONCLUSION

The proposed method described in the paper utilizes white light scanning interferometry to measure the thickness of the thin film. In the experimental setup, the amplitude Z value was found to be approximately constant at 3.4 rad, which closely matched the theoretical value. However, differences between simulation and experimental results were observed, attributed to various sources of noise such as aircon effects, vibrations, and ambient sound, as well as time gaps between measurements. When investigating the amplitude error values in the presence of random noise, it was noted that the errors introduced were also random in nature. Despite these challenges, the method proved effective in measuring the thickness of a transparent plate with a thin film on the top surface. By employing the proposed method, it became feasible to simultaneously measure the surface shape and thickness of the thin film, thereby reducing both the cost and time associated with the measurement process. This underscores the significance of the proposed technique in facilitating accurate and efficient characterization of transparent films.

AUTHOR CONTRIBUTIONS

This study mainly focuses on Transparent Film Profiling and Analysis by White Light Scanning Interferometry. The theoretical analyses on mathematical modeling for this study play a vital role in enhancing the high performance of White Light Scanning Interferometry for future nano-technology. This work could be provided to find the solution for research problems in advanced White Light Scanning Interferometry under the nano-technology and nano-science in reality.

ACKNOWLEDGMENT

The author also wishes to extend her special thanks to research collaborator Prof. Dr. OSAMI SASAKI from the Faculty of Engineering of Niigata University. The author wishes to express her gratitude to all persons who helped directly or indirectly towards the successful completion of this paper. Finally, the author wishes to express her special thanks to her parents, for their support and in Japan for their kind guidance and support to complete this research work without difficulties. Appreciation for colleagues from the Interferometer Research group under the Department of Electronic Engineering at Yangon Technological University.

REFERENCES

[1] G. Rendina, Experimental Methods in Modern Biochemistry, Philadelphia, PA: W. B. Saunders Company, 1976.
[2] H. Fujiwara, Spectroscopic Ellipsometry: Principles and Applications, John Wiley & Sons Inc., 2007.
[3] D. Mansfield, "The distorted helix: thin film extraction from scanning white light interferometry," Proc. SPIE, vol. 2186, 2006.
[4] P. de Groot and X. de Lega, "Transparent film profiling and analysis by interference microscopy," Proc. SPIE, vol. 7064, pp. 706401-706406, 2008.
[5] S. Kim and G. Kim, "Thickness-profile measurement of transparent thin film layer by white-light scanning interferometry," Applied Optics, vol. 38, pp. 5968-5973, 1999.
[6] Y. Ghim, A. Suratkar and A. Davies, "Reflectometry-base wavelength scanning interferometry for thickness measurements of very thin wafers," Optics Express, vol. 18, no. 7, pp. 6522-6529, 2010.
[7] X. Jiang, K. Wang, F. Gao and H. Muhamedsalih, "Fast surface measurement using wavelength scanning interferometry with compensation of environmental noise," Applied Optics, vol. 49, no. 15, pp. 2903-2909, 2010.
[8] F. Gao, X. Jiang, H. Muhamedsalih and H. Martin, "Wavelength scanning interferometry for measuring transparent films of the fusion targets," Centre for Precision Technologies, University of Huddersfield, Huddersfield, HD1 3DH, UK.
[9] N. N. Hlaing, H. M. Tun, L. L. Y. Win, "Shape Measurement Analysis of Indium Tin Oxide Thin Film by Sinusoidal Phase Modulating Interferometry Techniques," in Proc. ISER Int. Conf., Singapore, 2-3 Feb. 2024.
[10] N. N. Hlaing, K. Z. Thet, A. Mon, T. T. Aung, T. T. New, W. K. Khaing, H. M. Tun, "Experimental Studies of Shape Measurement Thin Film By Interferometry Techniques," in Proc. ISER Int. Conf., Edmonton, Canada, 24-25 May 2020.
[11] K. Z. Thet, N. N. Hlaing, T. T. Aung, W. K. Khaing, T. T. Nwe, H. M. Tun, A. Mon, "Experimental Studies of Thickness Measurement For Thin Film By Interferometry Techniques," in Proc. ISER Int. Conf., Edmonton, Canada, 24-25 May 2020.



Nway Nway Hlaing is a dedicated academic professional currently serving as a Tutor or Demonstrator in the Department of Electronic Engineering at Yangon Technological University (YTU), situated in Gyogone, Insein, Myanmar. With a focus on fostering educational growth and contributing to the field of electronic engineering, she plays a crucial role in the academic and practical training of students at YTU. In this vibrant academic setting, she is involved in a variety of educational activities, including delivering lectures, conducting laboratory sessions, and guiding students through complex engineering concepts and applications. (email: manwaynwayhlaing.ytu@gmail.com).



Dr. Lei Lei Yin Win is a distinguished Professor in the Department of Electronic Engineering at Yangon Technological University (YTU), located in Gyogone, Insein, Myanmar. With a wealth of experience and expertise in the field of electronic engineering, she contributes significantly to the academic community at YTU through both teaching and research. She is instrumental in shaping the minds of future engineers. Her responsibilities include delivering advanced lectures, overseeing research projects, and mentoring students, thereby fostering a robust academic environment. Her research interests and contributions are well-regarded, making her a valuable resource for students and colleagues. (email: maleileiyinwin.ytu@gmail.com).



Dr. Hla Myo Tun is a Leading Pro-Rector for Research and Engineering Higher Education at Yangon Technological University (YTU), Myanmar. He specializes in professional training for Engineering Higher Education leaders, heads of departments, and faculty members. He also directs Research and Development programs and workshops and has worked as a certified Quality Assurance Evaluator of the Myanmar Engineering Council (MEngC). (email: kohlamyotun.ytu@gmail.com).



Mr. Devasis Pradhan working as an Assistant Professor in Grade 1 and Dean of Research and Development at Acharya Institute of Technology, Bengaluru, Karnataka, from 2017 onwards. His current research includes the effectiveness of 5G Green Communications, mmWave antenna design, UWB antennas, and its implementation. With 16+ years of experience in the Academic and Research field, he has published 76 research papers and eight papers submitted to IEEE Access and Reputed Book and 4 Authored Books and 3 Edited Books (CRC, ISTE, Bentham Science) with a reputed publishing house. (email: devasispradhan@acharya.ac.in).